Sensors and Actuators A 147 (2008) 52–59

Contents lists available at ScienceDirect

Sensors and Actuators A: Physical

journal homepage: www.elsevier.com/locate/sna

Direction finding of moving ferromagnetic objects inside water by magnetic anomaly

Yavuz Ege[a], Osman Kalender[b,*], Sedat Nazlibilek[c]

[a] Balikesir University, Necatibey Faculty of Education, Department of Physics, 10100 Balikesir, Turkey
[b] Turkish Military Academy, Department of Technical Sciences, 06100 Bakanliklar, Ankara, Turkey
[c] Communications and Electronics Systems Branch, 06100 Bakanliklar, Ankara, Turkey

ARTICLE INFO

Article history:
Received 7 November 2007
Received in revised form 14 January 2008
Accepted 3 March 2008
Available online 16 March 2008

Keywords:
Magnetic anomaly
Remote sensing
Magnetic measurement
Scanning systems

ABSTRACT

The remote sensing methods by the use of magnetic anomaly are gaining importance in applications of defense technologies and industrial purposes recently. In this study, it is aimed to determine the remote detection, the variation of characteristic of the voltage in the sensor relative to the motion, the effects of material length, magnetic permeability and direction of motion of the object on this characteristic and to convert them to a useful mathematical expression by using magnetic anomaly of ferromagnetic objects such as submarines moving inside water. For this purpose, first of all, a water tank of 1 m^3 is prepared and approximately a homogeneous magnetic field of 10^{-3} T is created within this water tank. Ferromagnetic materials with six different lengths and permeabilities are moved in three different directions relative to the position of the sensor by means of a computer controlled *x–y* scanner designed for this experiment inside this magnetic field. The magnetic change caused by this motion at the point where the sensor is positioned is detected as the output voltage of the sensor. A mathematical expression is formulated taken into account the variations of the sensor output voltage with respect to the length, magnetic permeability and the direction of motion of the material and it is validated by the experimental results. This study clearly shows that the existence and the direction of motions of ferromagnetic objects with different lengths and magnetic permeabilities inside water can be detected with high accuracy.

1. Introduction

The detection of submarines is possible by sonar systems sending acoustic waves and listening the reflected waves inside the water. However, the target submarines can also detect these waves. This is an undesirable way of detecting these kinds of vehicles in that kind of environment. In order to overcome this deficiency, another method that is effective and undetectable has to be found. One of the methods satisfying these requirements is the utilization of magnetic anomaly to detect submarines in a passive way that is especially crucial for military purposes.

Studies carried out to determine geometrical parameters such as position detection, depth or movement direction by using magnetic anomaly has been done since 1970 [1]. Basic approach on magnetic anomaly is based on the fact that any material is likely to disturb the structure of the magnetic field in which it locates. If this material moves within the magnetic field, the disturbance at the magnetic field also moves. However, while the active acoustic wave is disturbed by means of the effects such as turbulences in the sea, turbidity or multiple jumping, there would not be any structural changes in the magnetic field. Therefore, the works carried out to detect ships or submarines by magnetic anomaly are preferable [2,3].

Nevertheless, some of the ferromagnetic materials available in the earth can give rise to a background noise and interference signals on the sensor, evaluating the anomaly on the magnetic field in real time and performing this evaluation process in a differently defined field from the earth's magnetic field are necessary. On the other hand, the structure of the sensor used as well has to be simple, waterproof, insensitive to the background noise and high sensitive to the field [4–7].

In this work, first of all, we made a wooden water tank having the dimensions of 1 m × 1 m × 1 m. Two Helmholtz coils have been located on opposite sides of the tank. A nearly homogeneous magnetic field having an intensity of 10^{-3} T is created within the tank. We designed and built a computer controlled scanning system moving in the directions of *x* and *y* axes and having a step sizes in any desired distance resolution for moving the materials to be tested within the magnetic field inside the water tank. No ferromagnetic material that is likely to affect and disturb the magnetic

* Corresponding author.
E-mail address: okalender@kho.edu.tr (O. Kalender).

0924-4247/$ – see front matter © 2008 Elsevier B.V. All rights reserved.
doi:10.1016/j.sna.2008.03.010

Fig. 1. The testbed used for magnetic anomaly experimentation.

field has been used in the structures of both water tank and the x–y scanning system. Sensor to be used to detect the magnetic anomaly occurring because of the movement of the material inside the tank is located to the centre of the tank in order to be able for effectively observing the magnetic anomaly. The testbed designed, developed and used in our experiments is shown in Fig. 1.

The magnetic anomaly testbed is developed for the following purposes: (1) to detect remotely the ferromagnetic objects moving inside the water by the method of magnetic anomaly; (2) to determine the characteristic of voltage changes of the sensor with respect to the moving object; (3) to convert the data obtained for the effects of the length, permeability and the direction of the movement of the material on this voltage characteristic to a mathematical expression. Six different ferromagnetic objects having three different lengths and with three different permeabilities for each length are moved in three different directions relative to the location of the sensor. The data on the voltage changes of the sensor is recorded. Then, these voltage changes are plotted on graphs based on the locations of the moving object. The experimental results obtained are discussed in the following sections in detail.

In Section 2, the characteristic of the magnetic field created inside the tank is investigated and the homogenity is tested. Positioning the sensor and the effect of magnetic fields created by the Helmholtz coils at the location of the sensor on the sensor voltage are explained in Section 3. The effect of a moving product with a ferrous compound on the sensor voltage and the effects of the material length, the magnetic permeability and the movement direction again on the sensor voltage are discussed in Sections 4 and 5, respectively. At the last section, the results and the recommendations are presented.

2. Detection of the magnetic field inside the tank

First of all, we tried to understand that whether the magnetic field created by the magnetic field source within the scanning area is homogeneous or not. For this purpose, an ac signal with a frequency of 500 Hz and an amplitude of 10 V produced by an oscillator is applied to the Helmholtz coils in series following the amplifier stage and a magnetic field inside the water tank is produced. Then, a sensor coil having a number of turns of 11,000, a diameter of 0.5 cm and a length of 5 cm is fixed to the bar of the 2D scanner as perpendicular to the Helmholtz coils. The sensor coil is moved both in the x direction and the y direction with the steps of 10 mm in length at both directions, and the voltage across the sensor is determined. Then, the position of the coil is brought in parallel with the longitude of the Helmholtz by drawing the scanner system to the reset position. Again by moving the coil with the same steps, the variations on the voltage of the output of the sensor are measured. Hence, the variations of both magnetic fields between the Helmholtz coils have been determined. The variations of the voltages obtained in each direction are put in the formula given by $B = V/(4\pi N_2 A f)$ for the x and y directions and plotted as a three-dimensional graphs as shown in Fig. 2 by using the explanations in [8,9]. Notice the graphs that the magnetic field produced at the scanning area of about 1 m × 1 m has both x and y components. Furthermore, it is clearly seen that in which of the areas the x component and in which of the areas the y component of the magnetic field are dominant.

If we combine these two graphs by the superposition principle, we see that the magnetic field in the scanning area is nearly homogeneous.

3. Positioning of the sensor and the calculations in the sensor area

The best position for the sensor to be used for the purpose of the detection of the movement direction by magnetic anomaly is determined as the point T (500 mm, 425 mm) where the magnetic field, $B_{\parallel}$, stays at a fixed value based on the experimentation results carried out to understand the distribution of the magnetic field

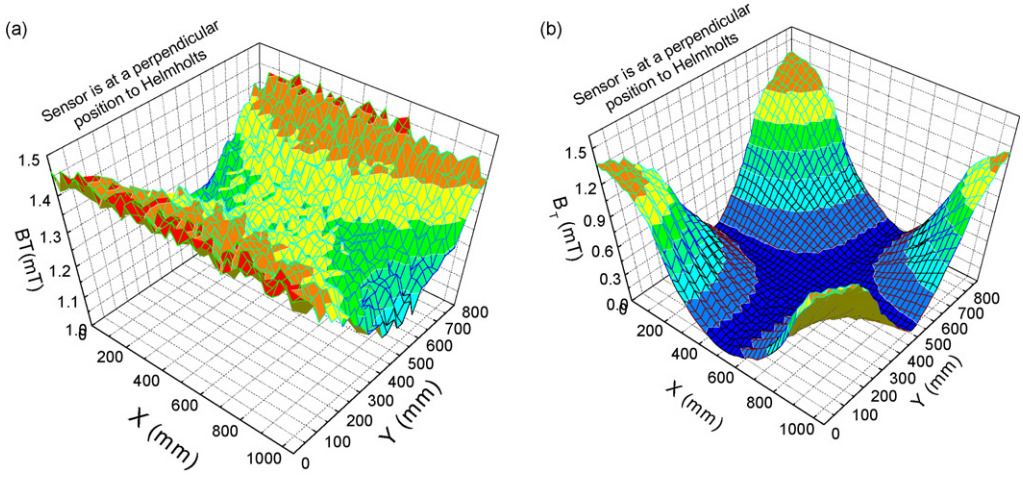

Fig. 2. The variations of the magnetic field in the scanning area (a) for x component and (b) for y component.

during the first step of our study as explained in Section 2 (see Fig. 2).

Two factors play an important role for selecting this point as the point where the sensor is positioned; namely, first, the $B_{\parallel}$ component is nearly homogeneous in this region and second, the magnetic anomaly effect created by the ferromagnetic product that is to be moved is high.

In our work, the sensor is fixed at the point T being in parallel with the Helmholtz coils. Because, rather than being perpendicular, the variations because of the magnetic anomaly in parallel positioned sensor can be higher than the variations in perpendicular case. But, in order to catch this high marked variation, the magnitude of the $B_{\parallel}$ magnetic field produced by Helmholtz coils at the point T is important. In our study, the variables affecting this field have been determined and based on this information the characteristic of the current to be applied to the Helmholtz has been ascertained. The total magnitude of the magnetic field at the point T is determined by means of the magnitude of the magnetic field created by a single rectangular turn of the Helmholtz at the point T. The magnitude of a magnetic field at a distance of $s/2$ from the centre of the rectangular coil is the sum of the magnetic fields produced by finite length of current carrying four wires at a distance of r from themselves. The magnetic field of any finite length of current carrying wire can be given by Eq. (1) depending upon the length of the wire L and the x and the y distances of the point where the magnitude of the magnetic field is to be found from the centre of the current:

$$B = \frac{\mu_0 i}{4\pi x}\left[\frac{y}{(x^2+y^2)^{1/2}} - \frac{y-L}{((y-L)^2+x^2)^{1/2}}\right] \tag{1}$$

The calculations of the magnitudes of magnetic fields B_1 and B_3 created by current carrying wires at the upper and the lower parts of the rectangular coil at the point T by the use of Fig. 3.

As seen from Fig. 3, for the upper wire:

$$k = \left[\frac{s^2+c^2}{4}\right]^{1/2}, \qquad r = \left[\frac{c^2+s^2+m^2}{4}\right]^{1/2}, \qquad x = k, \qquad y = \frac{m}{2}$$

By putting these values into Eq. (1), we can obtain the magnitude of the magnetic field created by the upper wire as in Eq. (2):

$$B_1 = \frac{\mu_0 i}{4\pi((c^2+s^2)/4)^{1/2}} \times \left[\frac{m/2}{((c^2+s^2+m^2)/4)^{1/2}} - \frac{(m/2)-m}{((c^2+s^2+m^2)/4)^{1/2}}\right] \tag{2}$$

If we apply the same procedure for the lower wire, we can obtain the same result for B_3.

The parallel components of these fields B_1 and B_3 to the surface of the rectangular coil cancel each other and only the perpendicular components $B_{1\perp}$ and $B_{3\perp}$ can contribute to the magnetic field at the point T as seen in Fig. 3. The magnitudes of $B_{1\perp}$ and $B_{3\perp}$ are equal to each other and one of which can be determined from Eq. (3) as follows:

$$B_{1\perp} = B_1\cos\varphi, \qquad B_{1\perp} = B_1\frac{c/2}{((c^2+s^2)/4)^{1/2}},$$

$$B_{1\perp} = \frac{\mu_0 i}{2\pi(c^2+s^2)}\frac{mc}{((c^2+s^2+m^2)/4)^{1/2}} \tag{3}$$

Similarly, the contributions of the current carrying wires at the left- and right-hand side to the magnetic field at the point T can be calculated by the use of Fig. 4.

As seen from Fig. 4, for the wire at the left-hand side:

$$p = \left[\frac{s^2+m^2}{4}\right]^{1/2}, \qquad r = \left[\frac{c^2+s^2+m^2}{4}\right]^{1/2}, \qquad x = p, \quad y = \frac{c}{2}$$

By putting these values into Eq. (1), we can obtain the magnitude of the magnetic field created by the wire at the left-hand side as in Eq. (4):

$$B_2 = \frac{\mu_0 i}{4\pi((m^2+s^2)/4)^{1/2}} \times \left[\frac{c/2}{((c^2+s^2+m^2)/4)^{1/2}} - \frac{(c/2)-m}{((c^2+s^2+m^2)/4)^{1/2}}\right] \tag{4}$$

If we apply the same procedure for the wire at the right-hand side, we can obtain the same result for B_4.

The parallel components of these fields B_2 and B_4 to the surface of the rectangular coil cancel each other and only the perpendicular components $B_{2\perp}$ and $B_{4\perp}$ can contribute to the magnetic field at the point T as seen in Fig. 4. The magnitudes of $B_{2\perp}$ and $B_{4\perp}$ are equal to each other and one of which can be determined from Eq. (5) as follows:

$$B_{2\perp} = B_2\cos\Theta, \qquad B_{2\perp} = B_2\frac{m/2}{((m^2+s^2)/4)^{1/2}},$$

$$B_{2\perp} = \frac{\mu_0 i}{2\pi(m^2+s^2)}\frac{mc}{((c^2+s^2+m^2)/4)^{1/2}} \tag{5}$$

Therefore, the magnitude of the magnetic field produced at the distance $s/2$ from the centre of the Helmholtz when the current i is passed through only a single turn becomes

$$B_t = B_{1\perp} + B_{2\perp} + B_{3\perp} + B_{4\perp} \quad \text{or} \quad B_t = 2(B_{1\perp} + B_{2\perp})$$

In other words, the total magnetic field B_t can be found from the expression given in Eq. (6):

$$B_t = \frac{\mu_0 i}{\pi}\frac{mc}{((c^2+s^2+m^2)/4)^{1/2}}\left[\frac{1}{m^2+s^2} + \frac{1}{s^2+c^2}\right] \tag{6}$$

If we consider that we have two Helmholtz coils with N_1 turns, the total field at the point T having a distance of $s/2$ from both of the Helmholtz is given by Eq. (7):

$$B_T = \frac{2\mu_0 i N_1}{\pi}\frac{mc}{((c^2+s^2+m^2)/4)^{1/2}}\left[\frac{1}{m^2+s^2} + \frac{1}{s^2+c^2}\right] \tag{7}$$

This expression is for the magnitude of the magnetic field at the point in air. If we consider that the sensor has a core with a magnetic permeability μ_1, the total magnitude of the field producing the voltage V_0 at the sensor is given by Eq. (8):

$$B_T = \frac{2\mu_1 i N_1}{\pi}\frac{mc}{((c^2+s^2+m^2)/4)^{1/2}}\left[\frac{1}{m^2+s^2} + \frac{1}{s^2+c^2}\right] \tag{8}$$

In accordance with the Faraday law, the voltage produced at the point T is also given by the expression in Eq. (9):

$$V_0 = N_2 A\frac{dB_T}{dt} \tag{9}$$

As it is known that the creation of the voltage V_0 at the sensor depends on the change in the flux of the magnetic field. The cause of change in the magnetic flux is the time varying current i applied to the Helmholtz. The variation of the current is sinusoidal with

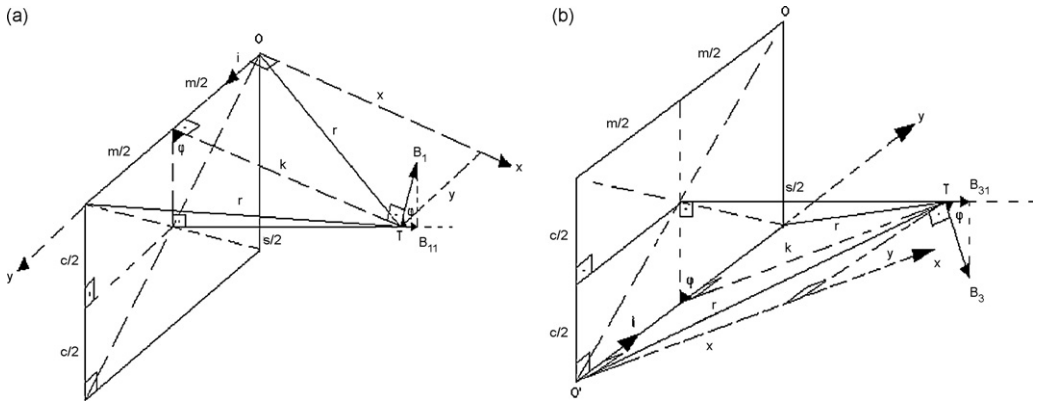

Fig. 3. Vectorial representation of magnetic fields B_1 and B_3.

respect to time, that is, $i = i_{max} \sin(\omega t)$. Therefore the voltage V_0 can be found by Eq. (10):

$$V_0 = \frac{2\mu_1 N_1 N_2 A}{\pi} \frac{mc}{((c^2+s^2+m^2)/4)^{1/2}} \left[\frac{1}{m^2+s^2} + \frac{1}{s^2+c^2}\right] \frac{di}{dt},$$

$$V_0 = 4\mu_1 N_1 N_2 A f i \frac{mc}{((c^2+s^2+m^2)/4)^{1/2}} \left[\frac{1}{m^2+s^2} + \frac{1}{s^2+c^2}\right] \quad (10)$$

Notice that we cannot say neither a voltage V_0 volts is read when the sensor is fixed in perpendicular to the Helmholtzs nor a voltage of 0 V is read when the sensor is fixed in parallel with the Helmholtzs. Since, as seen in Figs. 3 and 4, the magnetic field created by the Helmholtzs at the regions outside the point T clearly has both a perpendicular component and a parallel component. Therefore, if we locate a sensor coil with a specific length to a region the centre of which being the point T in parallel with the Helmholtzs, a voltage of V_1 is read from the sensor. The reason of this is the parallel component of the magnetic field in the immediate vicinity of the point T (around the coil).

Therefore, if the sensor coil is positioned in parallel with the Helmholtzs at the centre point T (500 mm, 425 mm), then a V_1 voltage is induced in the sensor coil, however if the sensor coil is positioned perpendicular to the Helmholtzs, then a V_2 voltage is induced in the coil. Hence the magnitudes of V_1 and V_2 voltages can be found by Eqs. (11) and (12) as follows:

$$V_1 = 4\mu_1 N_1 N_2 A f i \eta_1 \frac{mc}{((c^2+s^2+m^2)/4)^{1/2}} \left[\frac{1}{m^2+s^2} + \frac{1}{s^2+c^2}\right] \quad (11)$$

$$V_2 = 4\mu_1 N_1 N_2 A f i \eta_2 \frac{mc}{((c^2+s^2+m^2)/4)^{1/2}} \left[\frac{1}{m^2+s^2} + \frac{1}{s^2+c^2}\right] \quad (12)$$

where η_1 is the parallel component's factor and η_2 is the perpendicular component's factor. The value of η_1 is equal to either $(B_\parallel/(B_\perp^2+B_\parallel^2)^{1/2})$ or $(V_\parallel/(V_\parallel^2+V_\perp^2)^{1/2})$. In order to determine this factor experimentally in our study, the sensor at the point T is first positioned in parallel with and then perpendicular to the Helmholtz, and $V_\parallel$ versus $V_\perp$ values that are the effects of $B_\parallel$ versus $B_\perp$ at this point are found. These values can be seen from Fig. 2 as well. If these voltage values are put into the expression above, $\eta_1 = 0.104$ is found. Since $\eta_1 + \eta_2 = 1$, then $\eta_2 = 0.896$.

By means of Eq. (11), it had been determined how and by which variables the voltage to be established in the sensor would change while the sensor being in parallel with the Helmholtzs, and the current and the frequency values for which the most prominent effect of the sensor arised from the magnetic anomaly created by the movement of the ferromagnetic object are determined. It is found that the most appropriate values for the current is 0.5 A and the frequency is 500 Hz. By the utilization of these values, a magnetic field having a value of 0.338×10^{-3} T has been created at the point T (500 mm, 425 mm) as seen in Fig. 2.

After establishing the magnetic field as explained above, no changes have been done in the variables determining the magnitude of this field and hence the magnitude of the voltage V_1 throughout the experimentation. So it becomes possible to determine how the magnetic anomaly produced by the moving ferromagnetic object within the magnetic field affects the output voltage of the sensor. With the help of this, the movement direction of the ferromagnetic object is found.

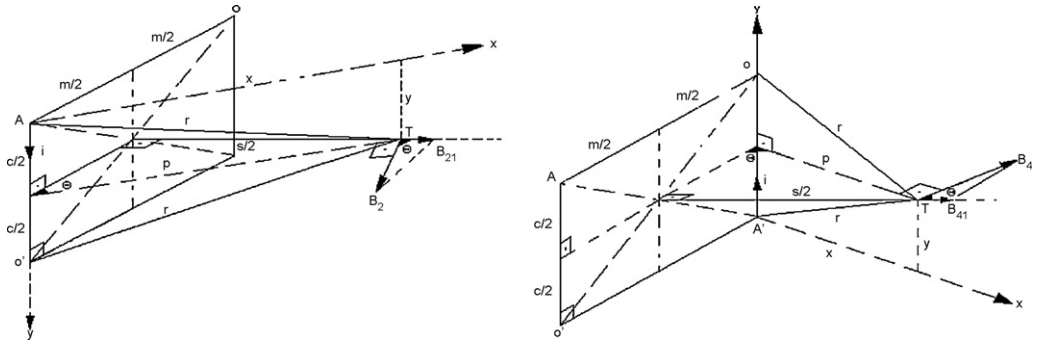

Fig. 4. Vectorial representation of magnetic fields B_2 and B_4.

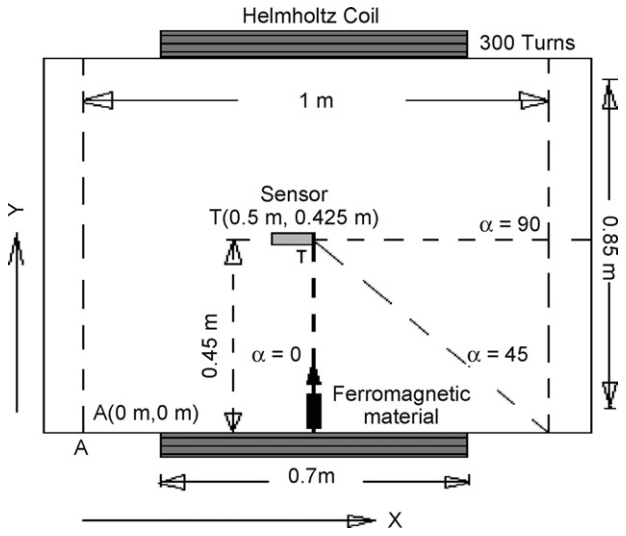

Fig. 5. Position of the sensor and motion types of the ferromagnetic object.

4. The effect of moving ferromagnetic objects in a defined magnetic field to the sensor output voltage

This is the second step of our study. Here we investigate the effect of moving ferromagnetic objects in a defined magnetic field to the sensor output voltage. For this purpose, three ferromagnetic objects with different length but having the same permeability and also three ferromagnetic objects with the same length but different in permeabilities are taken and each of them are moved one by one in the magnetic field produced by the Helmholtzs in three different directions.

Each object is first drawn along the x-axis for $x = 500$ mm and then is moved along the y-axis in 10 mm steps. The effect of the object to the sensor output voltage is determined. Then, the object is drawn along the y-axis for $y = 425$ mm and then is moved along the x-axis in 10 mm steps. The effect of the object to the sensor output voltage is again determined. Finally, the object is moved diagonally from the starting point by 20 mm steps in x direction and 30 mm steps in y direction (Fig. 5).

After the end of experiments, the sensor output voltage change obtained at the end of each different motion and for each object is converted to a graphical form. In Fig. 6, the changes created by the 3 cm × 4 cm × 30 cm M5 Si–Fe ferromagnetic object for every three motion is demonstrated.

As seen from Fig. 6, the direction of the ferromagnetic object can easily be understood from the output voltage variation of the sensor. There is no voltage variation only when the object moves in parallel with the x-axis. The reason for this is that the direction of anomaly occurred because of the moving object is perpendicular to the direction of the sensor motion.

In our study, all the experimental results obtained with the other objects have graphs similar to the characteristic variation shown in Fig. 6. This variation can be modelled as the following expression:

$$V = V_1 + \frac{A}{w\sqrt{\pi/2}}\, e^{((y-y_c)/w)^2} \tag{13}$$

where V_1 constant value can be found from Eq. (11). However, the parameters A, w and y_c are not constant but depend on the length of the ferromagnetic object, magnetic permeability and the direction of motion of the object. In our study, we determine the dependencies of these parameters (A, w and y_c) to the length of the ferromagnetic object, magnetic permeability and the direction of motion of the object, respectively (Fig. 7).

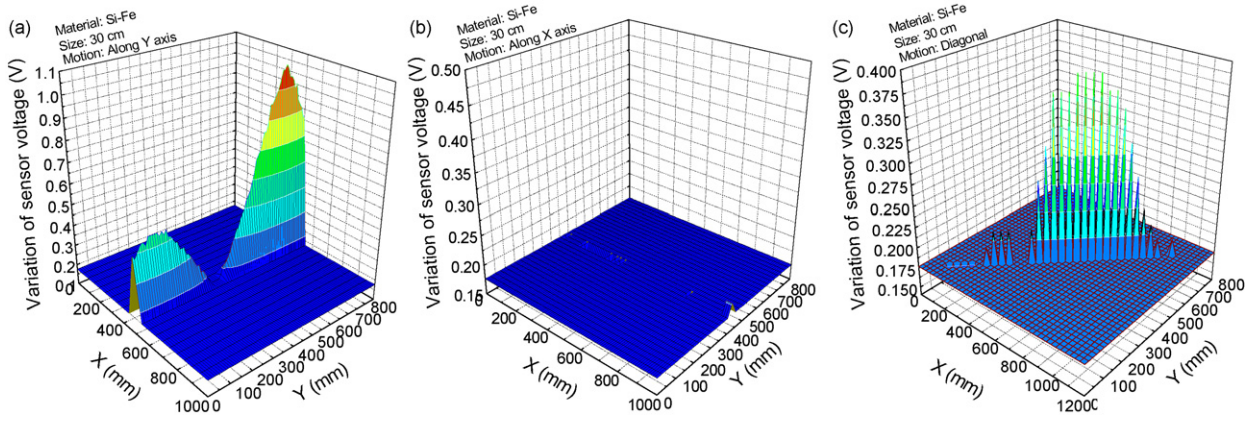

Fig. 6. The variations of the sensor output voltage by the motion of M5 Si–Fe in the field (a) along y-axis, (b) along x-axis, and (c) along diagonal line.

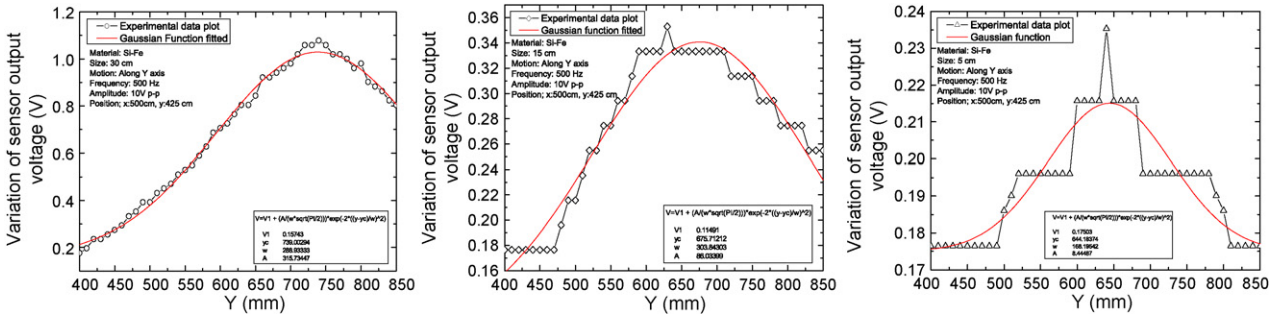

Fig. 7. The effect of the motion of three ferromagnetic objects in different lengths to the sensor output voltage.

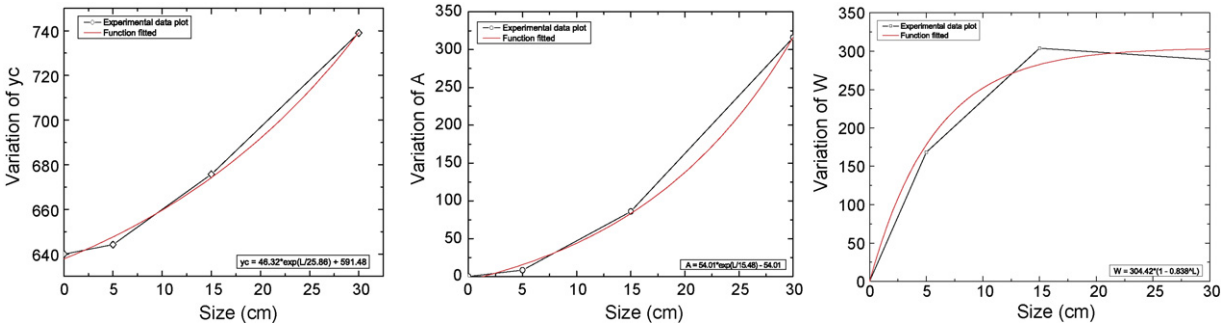

Fig. 8. The variation of the parameters y_c, A and w to the length of the ferromagnetic object.

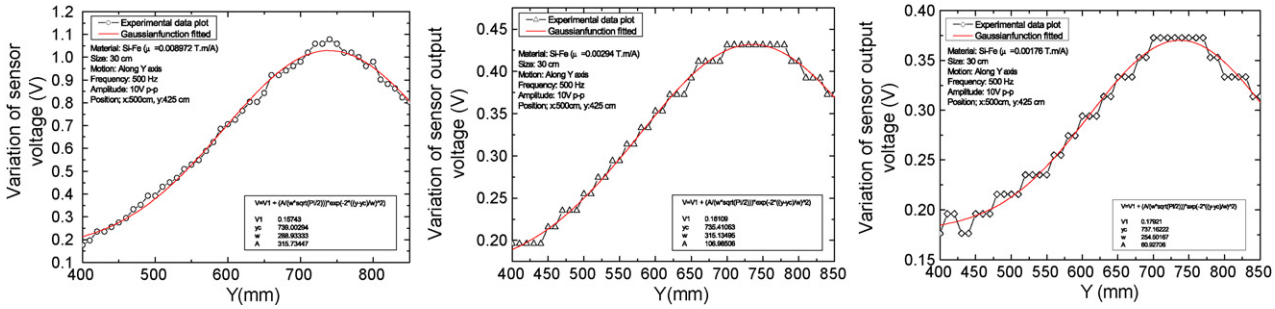

Fig. 9. The effects of the motions of ferromagnetic objects with three magnetic permeabilities along y-axis on sensor output voltage.

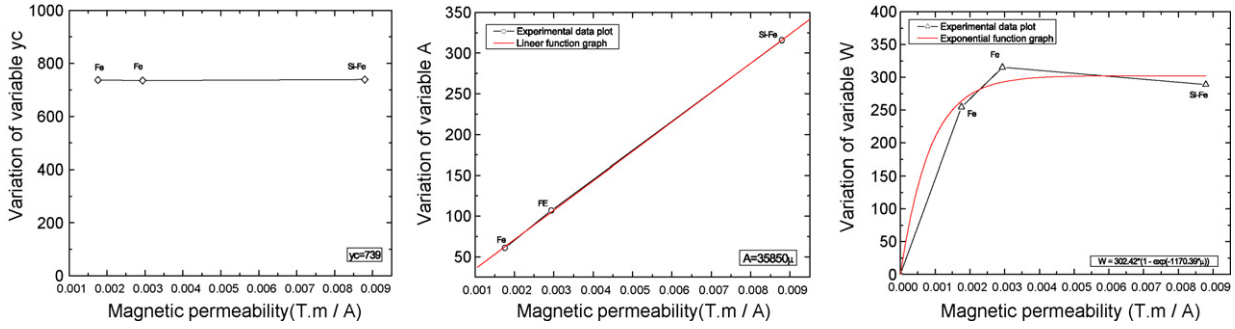

Fig. 10. Variations of y_c, A and w parameters with respect to the magnetic permeability of the object.

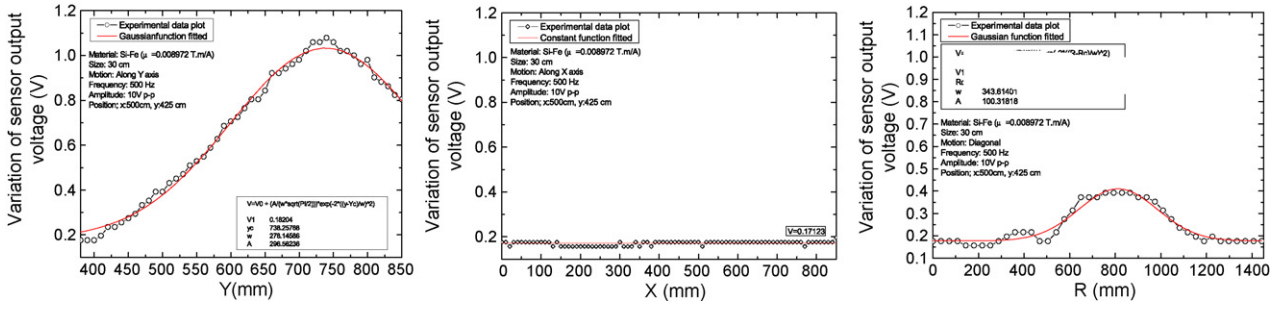

Fig. 11. The effects of the motions of the ferromagnetic product along three different directions to the output voltage of the sensor.

4.1. The effect of the length of a ferromagnetic object to the sensor output voltage

In this study, we analyse the sensor output voltage variations occurred during the motions of three M5 Si–Fe ferromagnetic objects in different lengths along the y-axis in order to be able to determine how the length of a ferromagnetic object effects A, w and y_c parameters. The variation characteristics of each object are as shown in Fig. 6. The change of the second peak with respect to the object length is determined. As the length of the object changes,

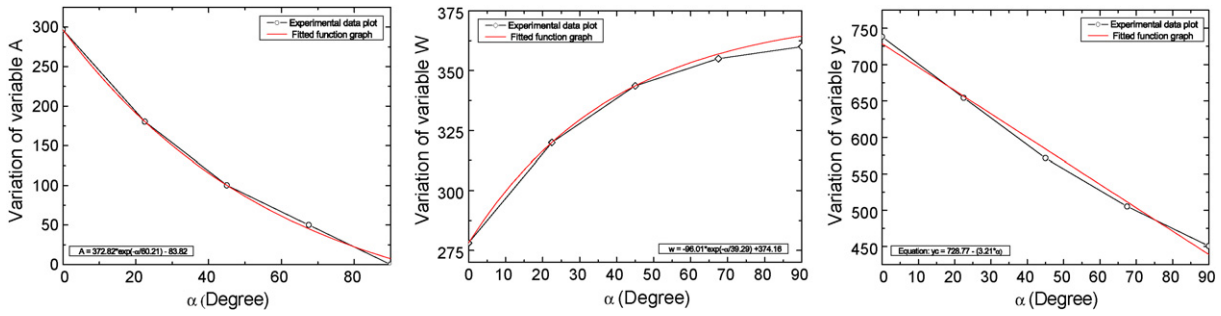

Fig. 12. The variations of the parameters A, w and y_c with respect to the direction of motion of the ferromagnetic object.

A, w and y_c parameters also change. In order to find the characteristics of these changes, the variations of each parameter with respect to object length are converted into graphical forms and a curve is fitted to each of the plots. The results are shown in Fig. 8.

As seen in Fig. 8, y_c and A parameters change with respect to the length of the object exponentially by the following equations:

$$y_c = 46.32\,e^{L/25.86} + 591.48, \quad A = 54.01\,e^{L/15.48} - 54.01$$

The parameter w changes with the length of the object as follows:

$$w = 304.42(1 - 0.838^L)$$

Table 1
The values of the variables for the defined magnetic field source

μ_1 (T m/A)	1.57×10^{-4}
N_1	300
N_2	11,000
A (m^2)	0.196×10^{-4}
f (Hz)	500
i (A)	0.1
η_1	0.104
m (m)	0.7
c (m)	0.4
s (m)	0.9

4.2. Dependency of the permeability of the ferromagnetic object on the sensor output voltage

In our study, in order to determine how the permeability of the ferromagnetic object changes the parameters A, w and y_c, three ferromagnetic objects in different permeability but in the same length are taken and moved along the y-axis. Then the variations at the sensor output voltage are analysed. The variation characteristics of all the three cases are as in Fig. 6a, the variation of the second peak in this graph with the permeability of the object is determined.

As seen in Fig. 9, A, w and y_c parameters show variations as the permeability of the ferromagnetic object lessens. In order to find the characteristics of these variations, each of the parameter's variation with respect to the magnetic permeability of the object is plotted as a graph and a curve is fitted. The results are shown in Fig. 10.

As seen in Fig. 10, the y_c parameter is not depended on the magnetic permeability of the object. The parameter A is a linearly changing. The parameter w shows an exponential variation.

4.3. Dependency of the sensors output voltage on the direction of the motion of ferromagnetic object

In the study, in order to determine the variations in A, w and y_c by the direction of motion of the ferromagnetic object, a Si–Fe ferromagnetic object with 30 cm has been moved from y-axis to x-axis in five different directions and the sensor output voltage variations obtained has been analysed. The characteristics of the variations of each motion are as in Fig. 6, the variation of the second peak in the graph has been determined.

As seen in Fig. 11, when the direction of motion of the ferromagnetic object is along the y-axis, the sensor voltage V_1 remains constant and the characteristics behaviour in other positions continues. In order to find the dependencies of the parameters A, w and y_c in the characteristic equation of behaviour on the direction of motion of the object, the variation of each parameter with respect to the direction of motion of the object is plotted and a curve is fitted to these graphs. The results are shown in Fig. 12.

As seen in Fig. 12, the parameter y_c is inversely proportional to the direction of motion, A decreases exponentially with respect to the direction of motion. The parameter w increases exponentially. Therefore, the variation of voltage on the sensor according to its position by a ferromagnetic object moving along a certain direction in a defined magnetic field and having a known magnetic permeability and length can be calculated by the following expression:

$$V = 4\mu_1 N_1 N_2 A f i \eta_1 \frac{mc}{((c^2+s^2+m^2)/4)^{1/2}} \left[\frac{1}{m^2+s^2} + \frac{1}{s^2+c^2}\right] + \left[\frac{(54.01\,e^{(L/15.48)} - 54.01)35,850\mu(372.82\,e^{-(\alpha/60.21)} - 83.82)}{304.42(1-0.838^L)(302.42(1-e^{-\mu 1170.39}))(-96.02\,e^{-(\alpha/39.29)} + 374.16)\sqrt{\pi/2}}\, e^{(g/d)^2}\right],$$

$$g = y - [((46.32\,e^{(L/25.86)}) + 591.48)739(778.77 - (\alpha \times 3.218))],$$

$$d = 304.42(1 - 0.838^L)302.42(1 - e^{-\mu 1170.39})(-96.02\,e^{-(\alpha/39.29)} + 374.16) \quad (14)$$

By means of this equation that is derived from the sensor voltage values experimentally measured, we can find the unknown variable of an object, whose only the direction or the length or the magnetic permeability is unknown, based on the sensor voltage value measured. In addition, in Eq. (14), the constant term representing the first term of the sensor output voltage is measured by the specific test setup is 0.196 V and can also be found by using the variables of our test setup (Table 1).

5. Conclusion and recommendations

The magnetic anomaly measurement system developed in our study shows that the direction of motion of the objects containing ferromagnetic materials such as iron, nickel and cobalt moving inside a magnetic field that is approximately homogeneous can be found by sensing the magnetic anomaly caused by this motion. As seen in Eq. (14), the magnitude of the output voltage of the sensor depends on the external magnetic field intensity, length of the ferromagnetic object, magnetic permeability of the ferromagnetic object, and the direction of motion of the object. Therefore, the longer the length and greater the magnetic permeability of the moving magnetic product, the greater the anomaly produced in the magnetic field and therefore the higher the output voltage of the sensor.

In the light of the experimental results, we can conclude that a lot of practical applications make use of this technique. For example, we can use this method for determining the direction of motion of a submarine moving in restricted or controlled areas. If we locate several sensitive magnetic sensors and defined magnetic sources at certain locations belonging to the possible route of the submarine, we can find the direction of motion of the submarine. However, the effects of the variables such as the length of the object, magnetic permeability of the material and direction of motion effecting the sensor voltage inside the magnetic field constituted on the output voltage of the sensors have to be determined as in Eq. (14) before hand. When the value of the voltage detected on the sensors because of the passage of the submarine, the length of the submarine and the values of the magnetic permeability are put on the equation, the direction of the motion of the submarine can be determined.

If we locate such a measurement system in a region where a submarine can only be moved in one direction and if we put the measured sensor voltage, length and direction values in the predetermined equation as known values, then we can find the only unknown variable, that is, the magnetic permeability of the material of the submarine. In such a way, we can determine very useful information on the submarine such as the direction of motion and the material from which it is produced, i.e. the signature of the submarine.

Acknowledgement

Authors specially thank to Olimed Ltd. Co., Balikesir for their support in this research.

References

[1] T.E. Tobely, A. Salem, Position detection of unexploded ordnance from airborne magnetic anomaly data using 3-D self organized feature map, Signal Processing and Information Technology, in: Proceedings of the fifth IEEE Int. Symp. (2005) pp. 322–327.
[2] C.L. Buchanan, Deep ocean search by visual, acoustic, and magnetic sensors, IEEE Trans. Audio Electroacoust. AU-19 (2) (1971) 124–132.
[3] A.S. Gadre, et al., An information-theoretic approach to underwater magnetic dipole localization, in: Proceedings of the MTS/IEEE OCEANS 2005, vol. 1, 2005, pp. 703–710.
[4] J.E. Lenz, A review of magnetic sensors, IEEE Proc. 78 (6) (1990) 973–989.
[5] M.J. Caruso, Applications of magnetoresistive sensors in navigation systems, in: Sensors and Actuators 1997, SAE SP-1220, 1997, pp. 15–21.
[6] G. Rieger, et al., GMR sensor for contactless position detection, Sens. Actuators A 91 (2001) 7–11.
[7] J.E. Lenz, A.S. Edelstein, Magnetic sensors and their applications, IEEE Sens. J. 6 (3) (2006) 631–649.
[8] D. Jiles, Introduction to Magnetizm and Magnetic Materials, Chapman & Hall, London, 1991, p. 56.
[9] O. Kalender, Y. Ege, A PIC microcontroller based electromagnetic stirrer, IEEE Trans. Magn. 43 (9) (2007) 3579–3585.

Biographies

Yavuz Ege received his BS and PhD degrees in 1995 and 2005, in Department of Physics Education, Necatibey Faculty of Education from Balikesir University, Balikesir, TR. He is currently working for Balikesir University, Department of Physics Education. His research interests are solid physics, magnetism and power electronics.

Osman Kalender received his BS and PhD degrees in 1986 and 2005, in Department of Electrical Education, Technical Education Faculty from Gazi University, Ankara, TR. He is currently working for Turkish Military Academy, Department of Technical Sciences. His research interests are generalized electrical machinery, power electronics and magnetism.

Sedat Nazlibilek received his BS degree in Department of Electric and Electronics Engineering from the Bosporus University, Istanbul, in 1984 and PhD degree in Department of Electric and Electronics Engineering from Middle East Technical University, Ankara, in 1992. He is currently working for Turkish General Staff Communications Electronics and Information Systems Division. His research interests are multisensors systems, robotics, system theory and magnetism.